NASA Technical Memorandum 84556

Flow Visualization in a Cryogenic Wind Tunnel Using Holography

A. W. Burner and W. K. Goad

NOVEMBER 1982

NASA

NASA Technical Memorandum 84556

Flow Visualization in a Cryogenic Wind Tunnel Using Holography

A. W. Burner and W. K. Goad
Langley Research Center
Hampton, Virginia

NASA
National Aeronautics
and Space Administration

Scientific and Technical
Information Branch

1982

SUMMARY

Results of holographic flow visualization are presented from tests made in the Langley 0.3-Meter Transonic Cryogenic Tunnel which was operated over a temperature range from 100 to 300 K and a pressure range from 1.1 to 4 atm. With holography, shadowgraph, schlieren, and interferometry could be attempted to determine the technique best suited for emphasizing the flow field. It was found that interferometry at the facility may be of limited use at the low-temperature—high-pressure conditions because of the jumbled nature of the reference fringes. The shadowgraph technique appears to be the best means of visualizing shocks at these high-density conditions where the shock was optically strong, and the increased sensitivity of schlieren was not needed to emphasize the shock. The spot size at the focus of the reconstructed beams was measured and used as an indicator of density fluctuations in the flow field. These density fluctuations appear to be caused by temperature fluctuations of the test gas which are relatively independent of tunnel conditions.

INTRODUCTION

The Langley 0.3-Meter Transonic Cryogenic Tunnel (0.3-m TCT) uses cryogenic gaseous nitrogen to simulate transonic flight conditions at a considerable power savings when compared with noncryogenic transonic facilities. With temperature as a test variable, the effects of aeroelasticity, Mach number, and Reynolds number can be separated, thus permitting testing not previously possible in conventional wind tunnels. The purpose of this paper is to report the first attempts at flow visualization in the 0.3-m TCT by using holography. The results of this study may also be applicable in the selection of flow visualization for the National Transonic Facility at the Langley Research Center, which also will use the cryogenic concept.

With holography, a high-resolution recording (hologram) is made during the flow. At a later time and at a location removed from the facility, it is possible to "reconstruct" from the hologram a duplicate of the optical light field which existed in the test section at the time of recording. Thus, different types of flow visualization, such as shadowgraph, schlieren, and interferometry, can be attempted to determine the technique best suited for emphasizing the desired flow phenomenon. Holography allows for optimization of each of these techniques since focusing, knife-edge adjustment, exposure level, etc., can all be varied during the reconstruction as opposed to these parameters being set before or during the data-recording phase, which is typical of conventional, nonholographic, flow-visualizaton methods.

Although density measurements are possible when using the shadowgraph and schlieren techniques, it is more common to use interferometry for quantitative density measurements since the change in density is represented by a change in interference fringe spacing or location rather than by a change in irradiance. Although determination from an interferogram of the density field for three-dimensional flows can be quite complicated or even impossible without prior knowledge of the density field or a multitude of views, the relationship between density and fringe shift for two-dimensional flows is quite simple. Thus, interferometry is particularly attractive for use with two-dimensional airfoil testing in the 0.3-m TCT. Although no

density measurements from interferograms are presented, the results of this study indicate where interferometry may be practical in the operating envelope of the facility.

SYMBOLS

K	Gladstone-Dale constant, cm^3/g
ℓ	distance from hologram to image of center of test section, cm
m	molecular weight, kg
n	refractive index
p	pressure, N/m^2
R	gas constant, J/kmol-K
T	temperature, K
Δ	change in variable
λ	wavelength, cm
μ	$= \lambda/\lambda_o$
ρ	density, g/cm^3
ϕ	optical power, 1/cm

Subscript:

o	parameter associated with hologram recording

FACILITY DESCRIPTION

The Langley 0.3-Meter Transonic Cryogenic Tunnel is a continuous-flow, fan-driven tunnel capable of cryogenic testing with gaseous nitrogen at transonic Mach numbers. (See ref. 1.) Cryogenic cooling is accomplished by direct injection of liquid nitrogen (LN_2) into the tunnel circuit with a cool-down or warm-up rate of 10 K/min or less. The tunnel, which is constructed of aluminum alloy and insulated with fiberglass mat, has a two-dimensional 20- by 60-cm test section which is encompassed by a rectangular pressure plenum. "D-shaped," schlieren-quality, fused-silica windows are mounted in the upper halves of the circular angle-of-attack turntables which are computer driven. These "D-shaped" windows are 1.9 cm thick and have a wedge angle of less than 30". The airfoil is centered on the circular turntable with its center line 1.9 cm below the lower edge of the windows. This whole assembly rotates as the angle of attack is changed.

The geometry of the "D-shaped" windows and of the airfoil section is depicted in figure 1. Note that the airfoil surface is not in the field of view of a collimated light beam which passes through the "D-shaped" windows. Two more windows are located in the pressure-plenum walls. These windows are 3.8-cm-thick, 22.9-cm-diameter,

schlieren-quality fused silica and have a wedge angle of less than 30". The NACA 0012 airfoil used for this study is a symmetrical airfoil having a maximum thickness of 12 percent of the chord. The ordinates of the airfoil section can be found in reference 2. The model for these tests had a 15.2-cm chord and 20.3-cm span.

The 0.3-m TCT is capable of operation at temperatures from 78 to 327 K, stagnation pressures from slightly greater than 1.0 to 6.0 atm, and Mach numbers from 0.05 to 0.95 (the maximum value being dependent on temperature.) The combination of cryogenic temperature and a pressure of 6 atm provides an extremely high Reynolds number at relatively low model loadings with considerably less power consumption when compared with conventional transonic tunnels. The unique ability to vary pressure and temperature independently of Mach number enables testing that was not previously possible with conventional tunnels.

EXPERIMENTAL ARRANGEMENT

The experimental arrangement (fig. 2) was similar to that of reference 3. A pulsed ruby laser, with intracavity aperture and a temperature-controlled etalon to ensure good spatial and temporal coherence, was used as the light source to record the holograms. A Pockels cell Q-switched the laser to produce up to 50 mJ of energy with a pulse width of 20 nsec at 694 nm. The combination of temperature gradients near the laser and wind-tunnel vibrations made it difficult to maintain laser alignment through the tests. The rear total reflector of the ruby laser was the only laser component not temperature controlled, and it needed realignment most often during the tunnel tests.

The ruby laser was mounted above the test section on an aluminum plate with a 6-mW He-Ne alignment laser mounted behind the rear reflector. Some of the optical components were mounted on the aluminum plate above the test section as well as on the aluminum angle and plates connected to two aluminum boxes which were attached to the sides of the pressure-plenum walls. Each box attached to the sides of the pressure plenum contained a parabolic mirror, having a 15-cm diameter and a 122-cm focal length, and an 8-cm-diameter flat mirror for folding the optical path. The boxes had several holes to vent dry room-temperature N_2 which was pumped into the boxes to prevent condensation on the optical surfaces inside as the tunnel temperature was lowered. A solenoid valve was used to stop the N_2 purge during the laser exposures. Thermocouples taped close to the plenum wall and at the ends of the boxes farthest from the tunnel were used to measure the temperature of the boxes during the tunnel runs.

The output beam of the ruby laser was first directed to a dielectric-coated beam splitter (the back surface was antireflection coated) which transmitted 50 percent of the beam power into the scene beam (a beam which traversed the pressure plenum and test-section windows) and reflected 50 percent of the beam power into the reference beam (a beam which passed over the tunnel). The beam splitter had a 30' wedge angle to reduce interference effects from the weak second-surface reflection. A spring-loaded adjustable mount, used initially for the beam splitter, was replaced with a positive locking mount during the tunnel tests to lessen the movement of the reflected reference beam because of vibration or wander of the spring-loaded mount.

The scene beam was directed by 99-percent-reflectivity, dielectric-coated mirrors with positive locking mounts to a 20× microscope objective and 25-μm pinhole, which together served as a combination of beam diverger and spatial filter. A solid-glass 0.7-neutral-density filter was placed in front of the microscope objective to reduce

the scene-beam irradiance at the hologram plane to 20 percent of the reference-beam irradiance. The spatially filtered and diverging scene beam passed through a 1-cm-thick window (with a 2.5-cm clear aperture) at the end of the aluminum box and was reflected from an 8-cm-diameter aluminum flat mirror to a parabolic aluminum reflector (with a 15-cm diameter and 122-cm focal length). Both reflectors were in mounts which could be adjusted from outside the aluminum box. The 25-μm pinhole was placed in the focal plane of the parabolic mirror to yield a collimated beam which traversed through the pressure-plenum and test-section "D-shaped" windows. The usable area of the collimated beam was limited by the lower edges of the "D-shaped" windows and by the copper-tubing purge lines located in the mounting boxes. (See fig. 3.)

After exiting the far-side pressure-plenum window, the collimated scene beam was collected and made to converge by another parabolic mirror having a 15-cm-diameter and and a 122-cm focal length. The converging scene beam was directed by an 8-cm-diameter flat mirror through a small window out of the box to a focus several centimeters past the window. The now-diverging scene beam was reflected by another flat mirror to the hologram plane.

After reflecting from the 50-50 beam splitter, the reference beam was directed over the tunnel to a 20× microscope objective. A pinhole was not used to filter the reference beam spatially since the long path length of the reference beam made it more susceptible to vibration or beam wander during a tunnel test. The focus of the microscope objective was placed at the focal point of a telescope doublet with 5-cm diameter and a 25-cm focal length to produce a collimated beam, which was then directed to the hologram plane for interference with the diverging scene beam.

The two-plate hologram holder used for recordings was a commercial unit having a fixed spacing of 0.7 cm between the two plates. The normal of the plate holder bisected the 40° angle between the scene and reference beams. The hologram plane was approximately horizontal since the scene and reference beams propagated in a vertical plane just before interfering at the hologram. The top and bottom plate positions of the holder were used for flow and no-flow recordings, respectively. Kodak holographic plates (10 by 13 cm), type 120-02, were used for the hologram recordings. To shield the hologram from stray light, the hologram holder was enclosed in a box with a 10-cm-diameter capping shutter on the bottom surface. The capping shutter was opened during a run just before a laser exposure was to be made. A hinged cover facilitated loading and unloading of the holograms from the plate holder. A photodiode located next to the reference-beam telescope doublet collected light diverged by the microscope objective to provide a monitor of the relative power of the ruby laser. The relative power was indicated by the amplitude of the photodiode signal, which was recorded on a high-speed storage oscilloscope.

RECONSTRUCTION OF WAVE FRONTS

In the experimental arrangement in the 0.3-m TCT an interference pattern due to the diverging, spherical-wave scene beam and plane-wave reference beam is recorded to form a hologram. (See fig. 4(a).) If the hologram is illuminated after development by a plane wave with geometry duplicating the recording, a diverging spherical wave (reconstructed scene beam) is diffracted from the hologram. If the hologram is illuminated from behind with a plane wave traveling in the opposite direction of the recording reference beam (conjugate reference beam), a converging spherical wave is diffracted from the hologram. (See fig. 4(b).)

Reconstruction with a conjugate reference beam (ref. 4) has some advantages over conventional reconstruction for this application. One advantage is that it produces a beam with a focus so that the schlieren technique can be attempted without the need for an additional beam focusing lens. A second advantage is that when reconstructing with the conjugate reference beam, the scene beam propagates in the opposite direction as in the recording. If a parabolic mirror of the same focal length and geometry as for the recording is used to collimate the backwards-propagating scene beam, the center of the test section is imaged without aberration (neglecting small window effects) and is focused at the same distance from the mirror as in the original recording. (See fig. 5.)

Local disturbances in the flow can be located by noting the position where the shadowgraph due to the disturbance is minimized. Assuming that the source of the disturbance is at the location where the shadowgraph effect is minimized is valid only if there are no other disturbances present in the scene beam for the recording. If several disturbances are present, the scene beam will suffer the integrated effect of all disturbances and the location where the shadowgraph effect is minimized will likely indicate the location of the last disturbance encountered by the scene beam.

During the period of the tunnel tests, holograms were reconstructed in a laboratory adjacent to the tunnel building to ensure that proper recordings had been made. A continuous-wave He-Ne laser with a wavelength of 633 nm was used as a light source to reconstruct the holograms originally recorded with a pulsed ruby laser with a wavelength of 694 nm. (After the tunnel tests were completed, an argon laser operating at 515 nm was used for reconstruction.) The disparity in wavelengths between recording and reconstructing causes a scale change as well as the introduction of aberrations into the reconstruction process. Scale changes occur since the optical power ϕ of a hologram scales as the ratio μ of the reconstructing wavelength λ to the recording wavelength λ_o, or

$$\phi = \mu\phi_o \tag{1}$$

where ϕ_o is the optical power of the hologram at λ_o. Thus, the focus of the reconstructed scene beam is located farther from the hologram for reconstruction at 633 nm than in the original recording. If a constructional ray parallel to the direction of propagation of the recording plane-wave reference beam is traced through the focus of the recording scene beam, the point of intersection of the ray and the hologram plane is the nodal point for the hologram. (See fig. 6.) During reconstruction at wavelength λ, the paraxial location of the focus is found by tracing a ray parallel to the reconstruction plane wave beam through the nodal point. The location of the intersection of the ray with the new image plane, which is at a distance of just $1/\phi$ from the hologram, determines the paraxial focus of the reconstructed scene beam. (See fig. 7.)

The formation of an image of the test section behind the hologram during the recording is depicted in figure 8. When reconstructing with a conjugate reference beam of wavelength λ, the image of the center of the test section is virtual and is located at a distance ℓ/μ from the hologram. By knowing the location of this virtual image, the location of the center of the test-section real image, which was formed by a parabolic mirror with a 122-cm focal length during reconstruction, can be determined.

Examples of the focusing capability of a holographic reconstruction are shown in figure 9. In figure 9(a) the film back is translated so that the focus is on a clamp which holds the purge tube ring on the hologram side of the setup. In figure 9(b) the focus is on the lower edge of the "D-shaped" window on the laser side of the setup. In figure 9(c) the focus is on the purge tube ring on the laser side of the setup. With these three convenient reference planes determined, the proper focus location could be verified.

RESULTS AND DISCUSSION

Holograms were made over a temperature range from 100 to 300 K and a pressure range from 1.1 to 4 atm. The Mach number was 0.77 for all tunnel tests except for those at 300 K and 4 atm at which the Mach number was limited to 0.65. The angle of attack was set at either 0°, 4°, or 8° for the tests. A reconstructed schlieren photograph and interferogram of flow made at 250 K and 2 atm is shown in figure 10. The schlieren photograph was produced by placing a vertical knife edge close to the focus of the reconstructed beam in order to emphasize the shocks. The interferogram was produced with the two-hologram method in which the reconstructed beam from a no-flow hologram is made to interfere with the reconstructed beam from a flow hologram. The relative orientation of the two holograms can be adjusted to shift the location and orientation of the reference fringes. The same flow hologram was used for both the schlieren photograph and the interferogram.

As the tunnel temperature was lowered, the shock became much more visible until a very broad dark band was noted at the shock location, even for a focused shadowgraph. At those conditions where the shock was optically strong, the best visualization was obtained with a focused shadowgraph and, thus, schlieren was not necessary for emphasizing the shock. Figure 11 shows a holographic reconstruction of a focused shadowgraph of flow at 100 K and 4 atm. Note the grainy appearance of the reconstruction and the very strong (optically) shock. Since the grainy structure of the reconstruction becomes smallest at a focus corresponding to the center of the test section, the disturbance causing this graininess most likely lies within the test section rather than in the plenum or outside the tunnel. (A similar graininess noted in ref. 5 was attributed to turbulence in the flow field.) The lowest temperature at which usable interferograms have been produced by using two-hologram interferometry is 125 K, although the interpretation of the interferogram would be difficult because of the excessive waviness of the fringes.

Figure 12 shows interferograms made in the 0.3-m TCT over a range of conditions. These interferograms were produced during the holographic reconstruction by directing the reconstructed collimated wave front to a glass plate which had a few seconds of wedge angle. The first and second surface reflections from the glass plate produced two laterally sheared wave fronts which interfered to produce, in the absence of a disturbance, straight-line fringes indicative of the amount of wedge (for collimated illumination). Although interpretation of laterally sheared interferograms can be difficult since a single shock now appears as two shocks, the relative insensitivity of the reference fringes to the setup geometry makes the technique useful when comparisons are desired. The location of the center of the photographs on the graph represents the tunnel flow parameters, total temperature, and pressure for that photograph. Equal-density lines are also drawn on the graph for comparisons. The interferogram labeled "test shot" at the lower left corner of the figure was made with the tunnel at 100 K and 1.5 atm with a Mach number of about 0.1. The interferogram labeled "test shot" at the lower right corner was made with the fan off at 300 K and 1 atm.

Figure 12 illustrates that the interference fringes become more jumbled and difficult to distinguish as the temperature is decreased or the pressure is increased. The fact that the effect is not simply due to an increase in density can be noted by comparing the interferogram at 300 K and 4 atm with the one at 150 K and 2 atm. Even though the density is the same for the two interferograms, the interferogram at 150 K and 2 atm is more jumbled than the one at 300 K and 4 atm.

Optical techniques for flow visualization respond to changes in the refractive index across the field of view. With interferometry the response is a variation in the position of reference fringes, whereas for a schlieren or shadowgraph the response is a variation in irradiance on the viewing plane. The change in refractive index Δn is directly proportional to the change in density. Thus,

$$\Delta n = K \, \Delta \rho \tag{2}$$

where K is the Gladstone-Dale constant. Changes in density can occur because of small fluctuations in temperature or pressure. For an ideal gas this relation is

$$\Delta \rho = \frac{m}{R}\left(\frac{\Delta p}{T} - \frac{p}{T^2}\,\Delta T\right) \tag{3}$$

Any changes in density caused by pressure variations are inversely proportional to the absolute temperature. Changes in density caused by temperature variations are proportional to the pressure divided by the square of the absolute temperature. Thus, for constant Δp and ΔT, $\Delta \rho$ due to small pressure variations would be 3 times greater and $\Delta \rho$ due to small temperature variations would be 36 times greater at 100 K and 4 atm than at 300 K and 1 atm. If the response due to an optical flow-visualization technique is plotted against both $1/T$ and p/T^2, it may be possible to determine whether the response is due primarily to temperature or to pressure fluctuations in the flow. If, for example, the density variations are due primarily to pressure fluctuations, then the optical response at different pressures and temperatures correlates better when plotted against $1/T$ than when plotted against p/T^2.

For this series of runs, a convenient parameter (optical response) that can be plotted against $1/T$ and p/T^2 is the spot size at the focus of the reconstruction. This spot size is defined to be the beam width which contains 80 percent of the beam energy and is found by scanning the focus with a knife edge at a known constant velocity. Measurement of the rise time of the signal from a photodetector located behind the knife edge then determines the spot size. Plots of spot size against $1/T$ and p/T^2 (normalized to 1 atm and 300 K) are presented in figure 13. Note that the correlation of spot size is much better when plotted against p/T^2 than when plotted against $1/T$, which indicates that the density variations across the flow may be largely due to temperature fluctuations rather than to pressure fluctuations. The linearity of the plot of p/T^2 also suggests that the temperature fluctuation (which is proportional to the slope) is relatively independent of tunnel conditions.

CONCLUDING REMARKS

Holographic flow-visualization tests have been made in the Langley 0.3-Meter Transonic Cryogenic Tunnel over a temperature range from 100 to 300 K and a pressure range from 1.1 to 4 atm. A graininess and jumbling of fringes and an increased spot size of the focused reconstruction were noted as the temperature was lowered and the pressure was increased. The density variations which produce these effects appear to be due to temperature fluctuations in the test-section flow rather than to pressure changes. At the high-density conditions, the shadowgraph technique appears to be the best means of visualizing shocks in the flow field.

Langley Research Center
National Aeronautics and Space Administration
Hampton, VA 23665
October 5, 1982

REFERENCES

1. Ray, Edward J.; Ladson, Charles L.; Adcock, Jerry B.; Lawing, Pierce L.; and Hall, Robert M.: Review of Design and Operational Characteristics of the 0.3-Meter Transonic Cryogenic Tunnel. NASA TM-80123, 1979.

2. Jacobs, Eastman N.; Ward, Kenneth E.; and Pinkerton, Robert M.: The Characteristics of 78 Related Airfoil Sections From Tests in the Variable-Density Wind Tunnel. NACA Rep. 460, 1933.

3. Burner, A. W.; and Goad, W. K.: Holographic Flow Visualization at NASA Langley. Instrumentation in the Aerospace Industry - Volume 25. Advances in Test Measurement - Volume 16, Part Two, Instrum. Soc. America, c.1979, pp. 477-484.

4. Collier, Robert J.; Burckhardt, Christoph B.; and Lin, Lawrence H.: Optical Holography. Academic Press, Inc., 1971.

5. Belz, R. A.; and Menzel, R. W.: Particle Field Holography at Arnold Engineering Development Center. Opt. Eng., vol. 18, no. 3, May-June 1979, pp. 256-265.

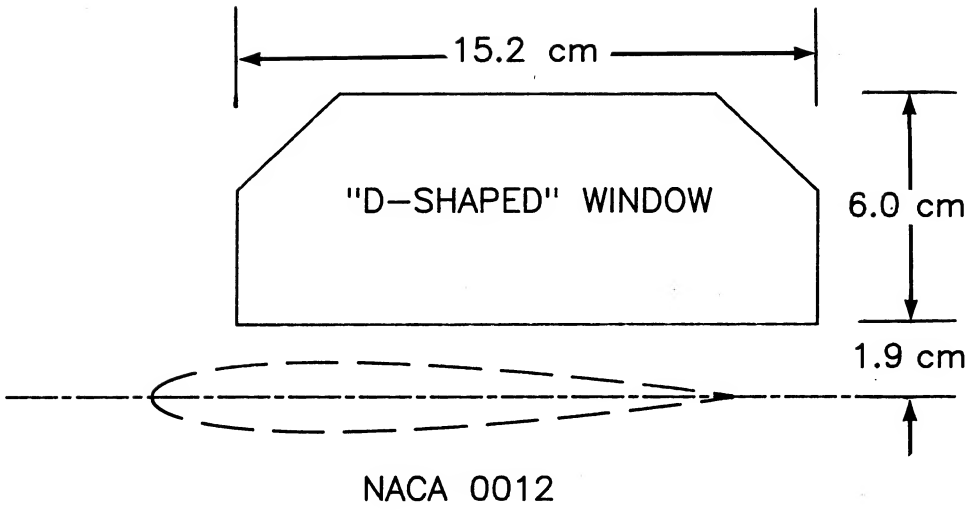

Figure 1.- Geometry of "D-shaped" windows and of NACA 0012 airfoil used for this study.

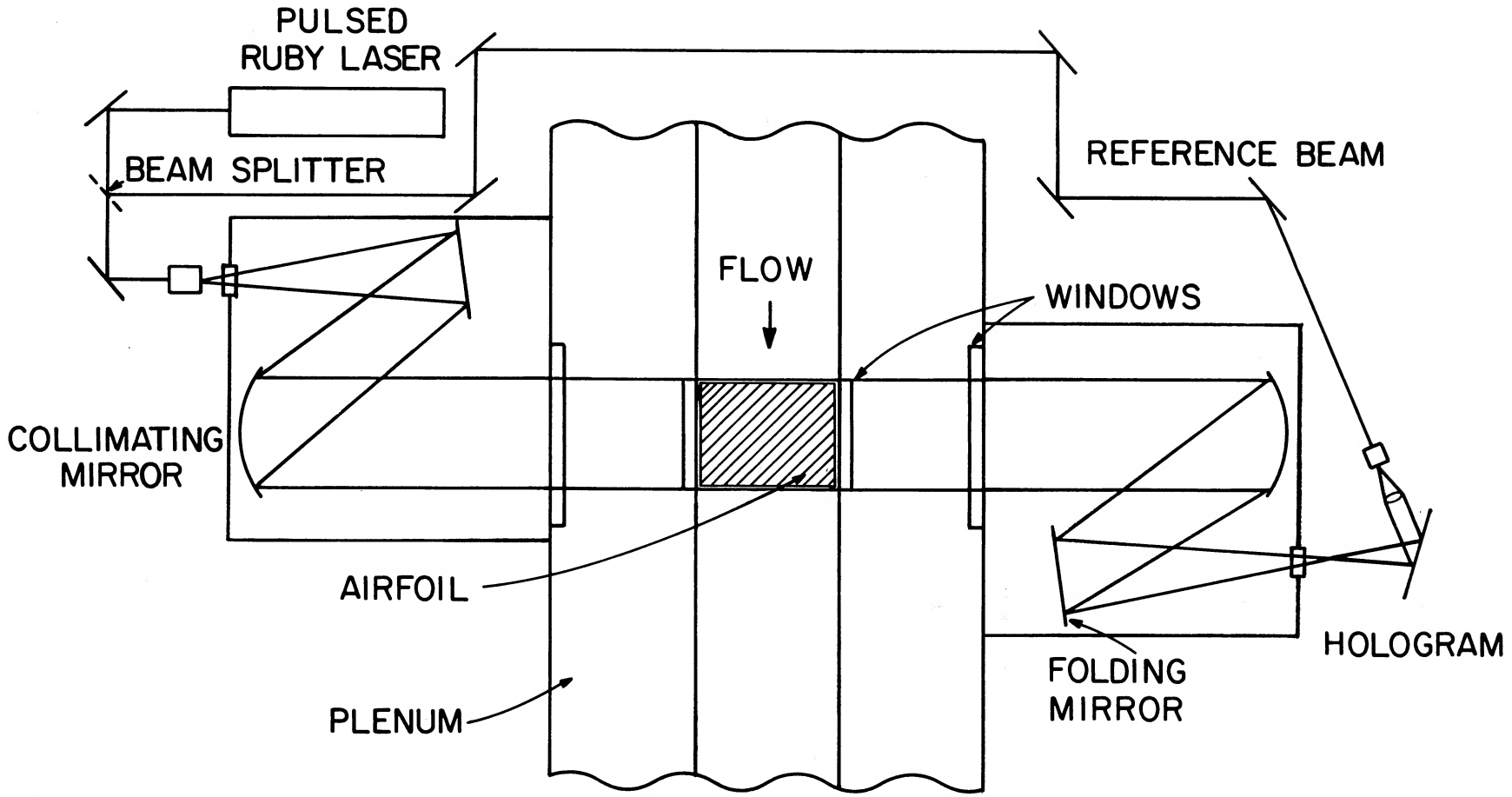

Figure 2.- Schematic drawing of holographic system in the 0.3-m TCT.

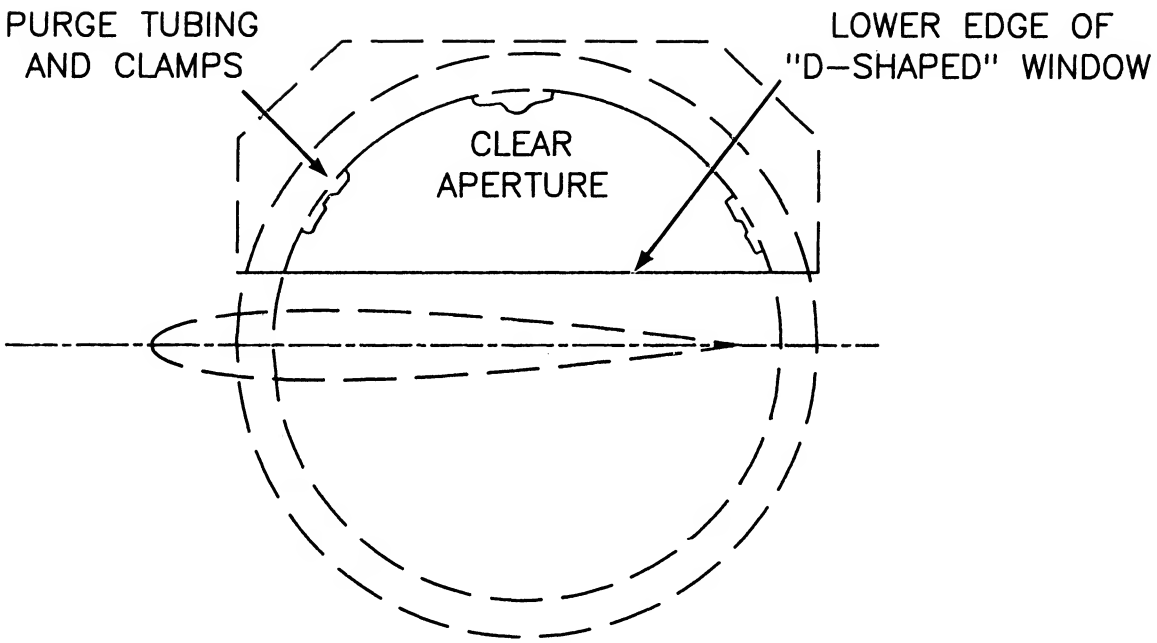

Figure 3.- Sketch illustrating clear aperture of flow-visualization system.

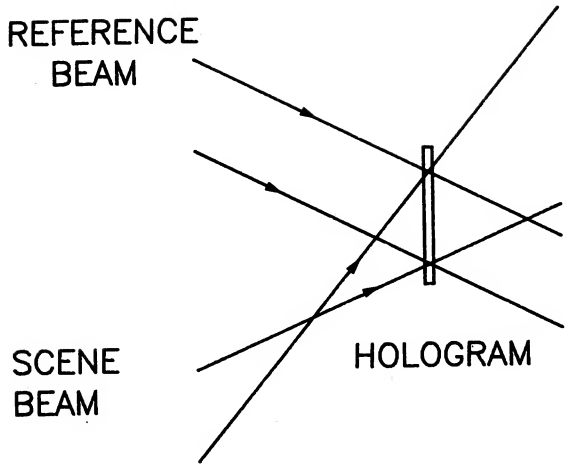

(a) Recording.

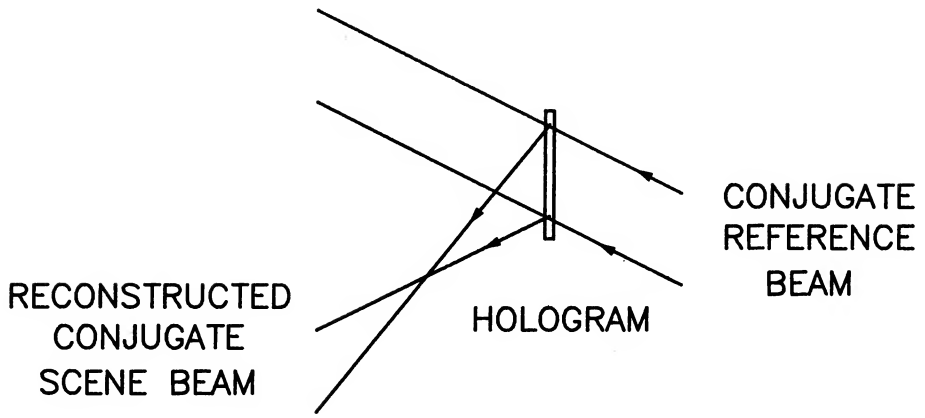

(b) Reconstruction with conjugate reference beam.

Figure 4.- Recording of hologram and reconstruction with conjugate reference beam.

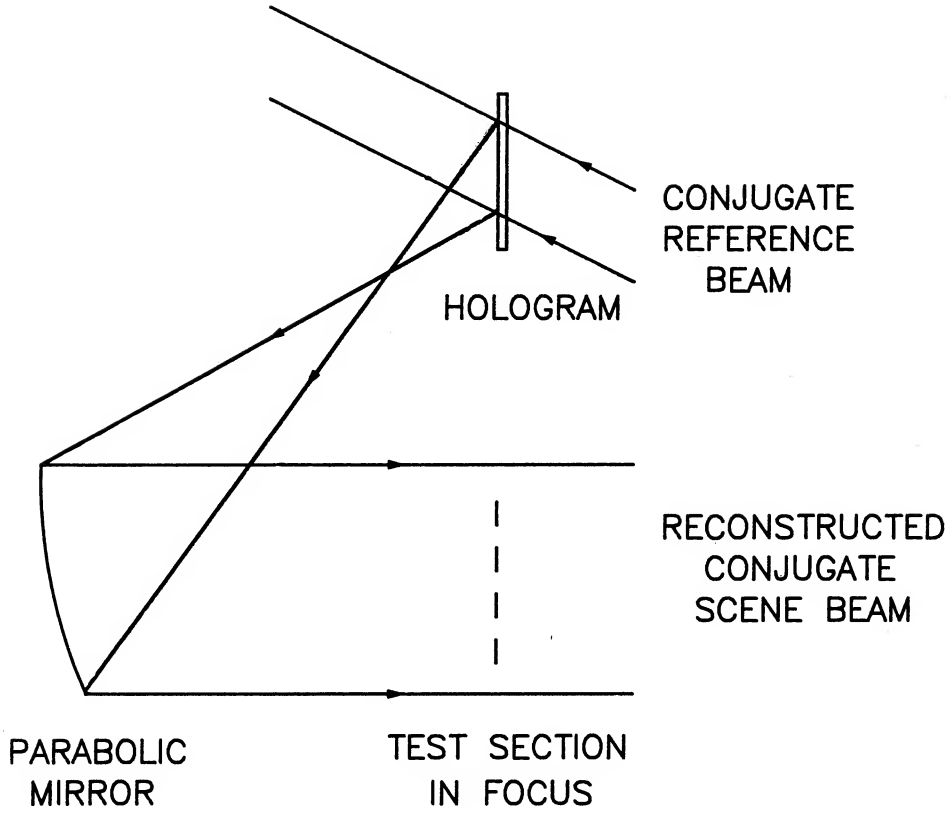

Figure 5.- Location of test-section image formed by parabolic mirror with conjugate reference beam.

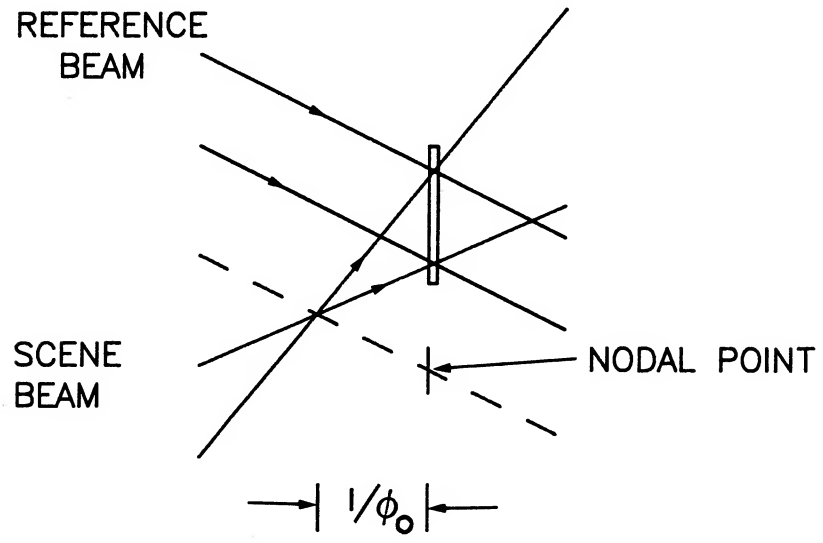

Figure 6.- Recording of hologram at λ_o.

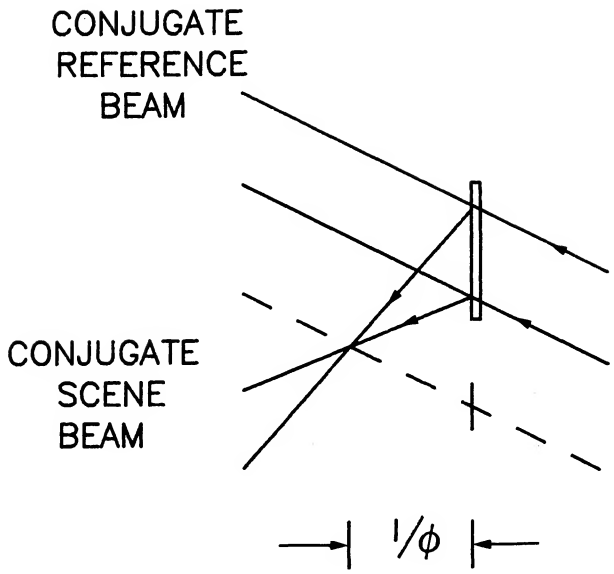

Figure 7.- Reconstruction at λ with conjugate reference beam.

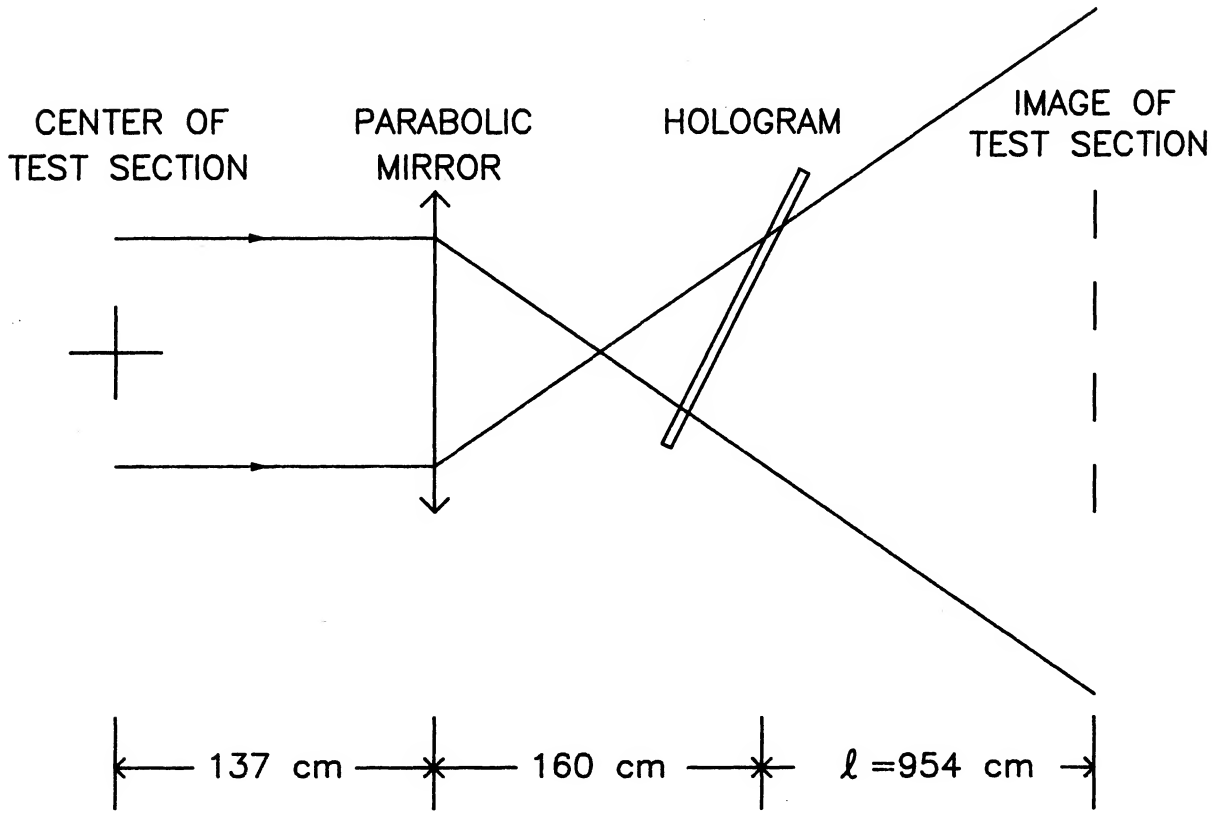

Figure 8.- Scene beam (unfolded) during recording of hologram. Not drawn to scale.

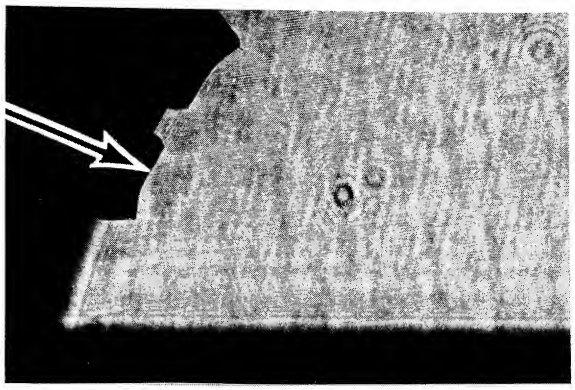

(a) Focused on tubing clamp nearest hologram.

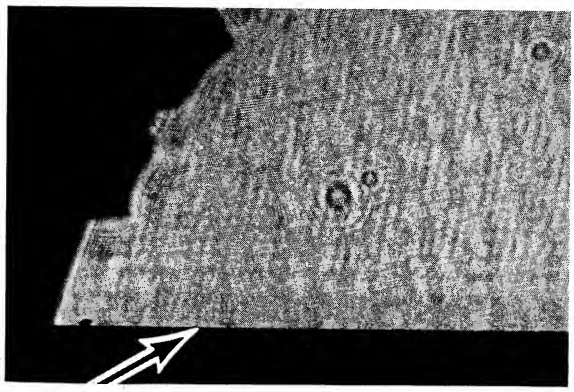

(b) Focused on "D-shaped" window nearest laser.

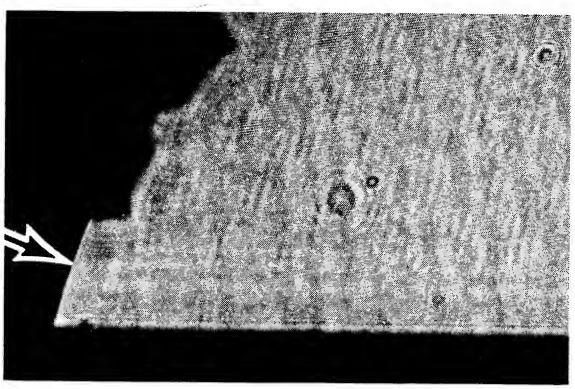

(c) Focused on tubing nearest laser.

L-82-177

Figure 9.- Reconstructions of a single no-flow hologram focused on three different planes.

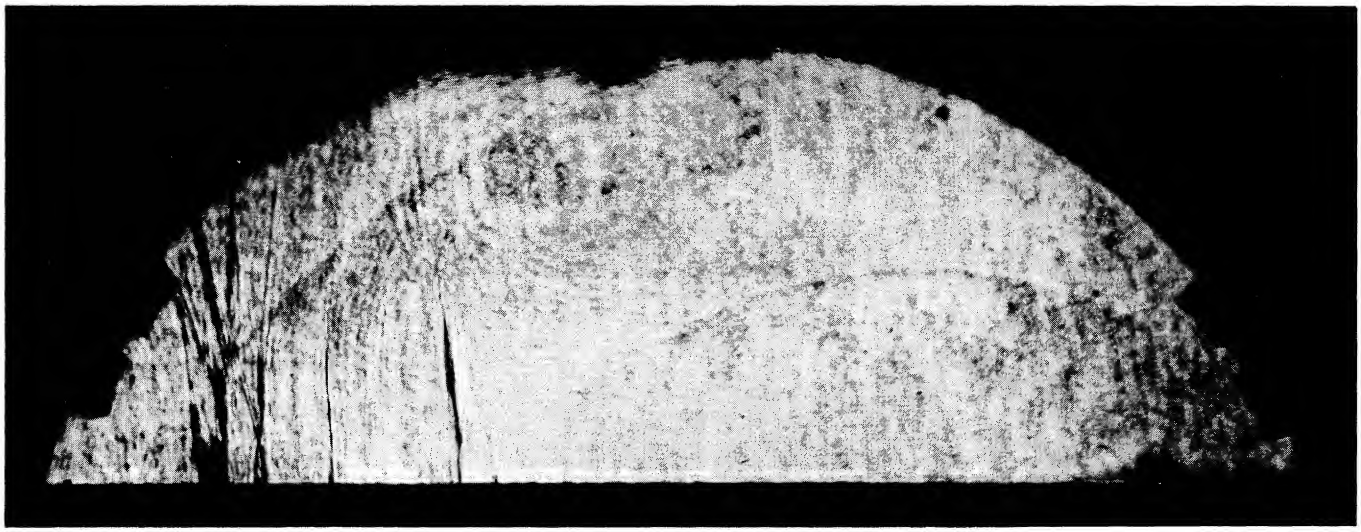

(a) Schlieren photograph.

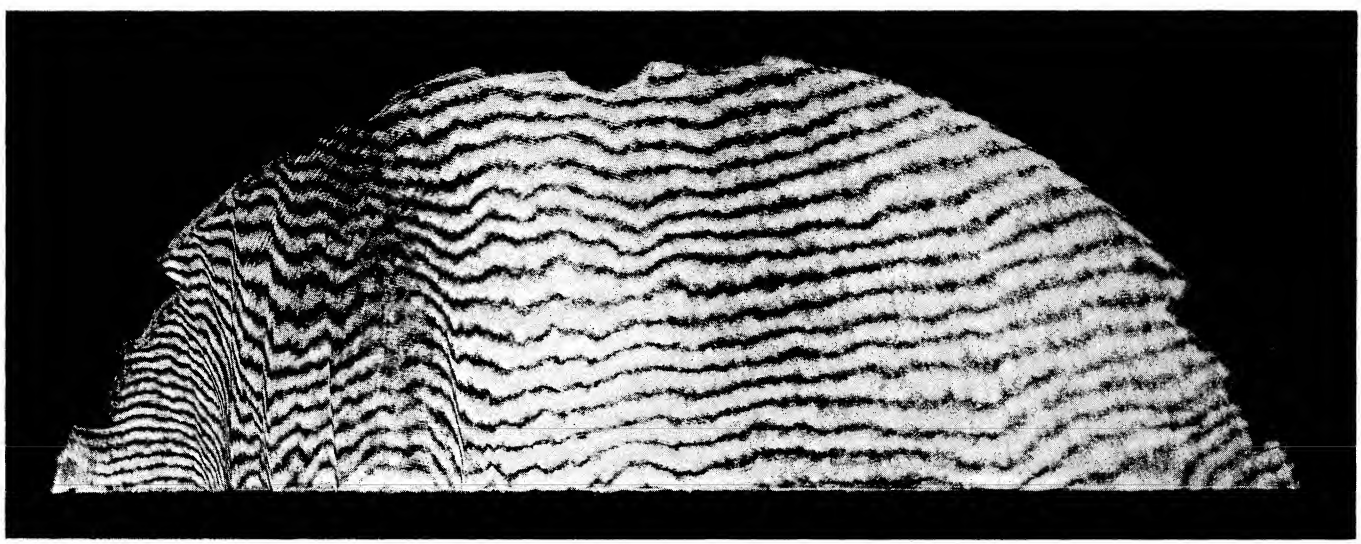

(b) Interferogram.

L-82-178

Figure 10.- Holographic schlieren photograph and interferogram of flow at 250 K and 2 atm at a Mach number of 0.77. Flow is from left to right.

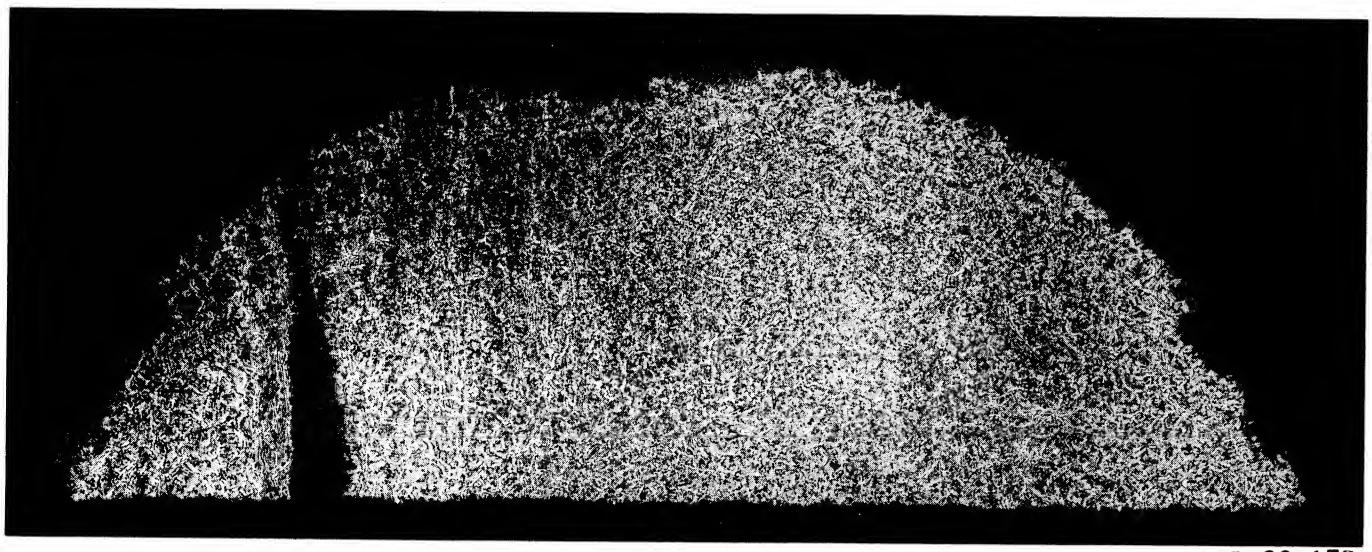

L-82-179

Figure 11.- Holographic shadowgraph at 100 K and 4 atm at a Mach number of 0.77. Flow is from left to right.

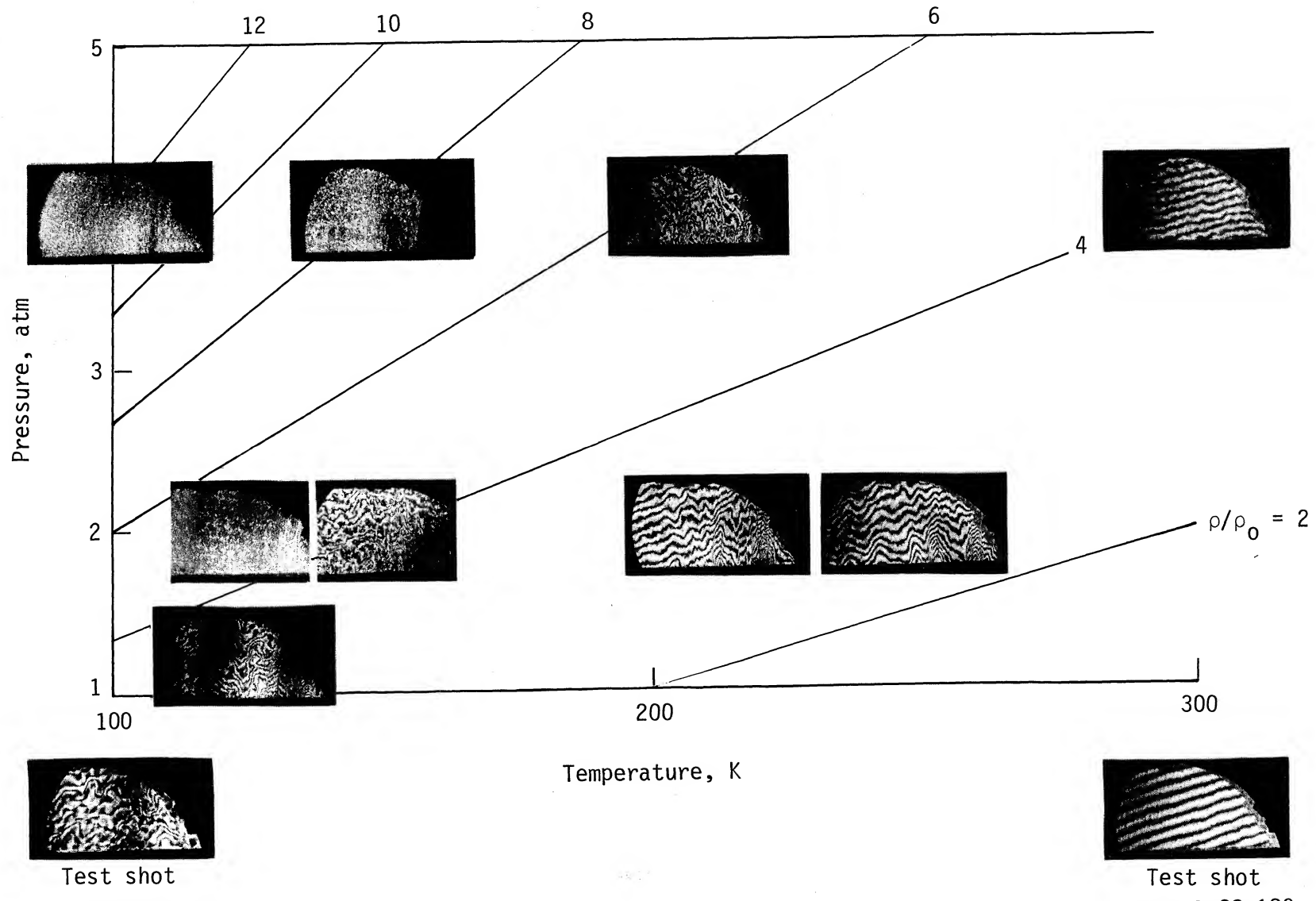

Figure 12.- Reconstructed shearing interferograms over a range of test conditions in the 0.3-m TCT. Flow is from right to left.

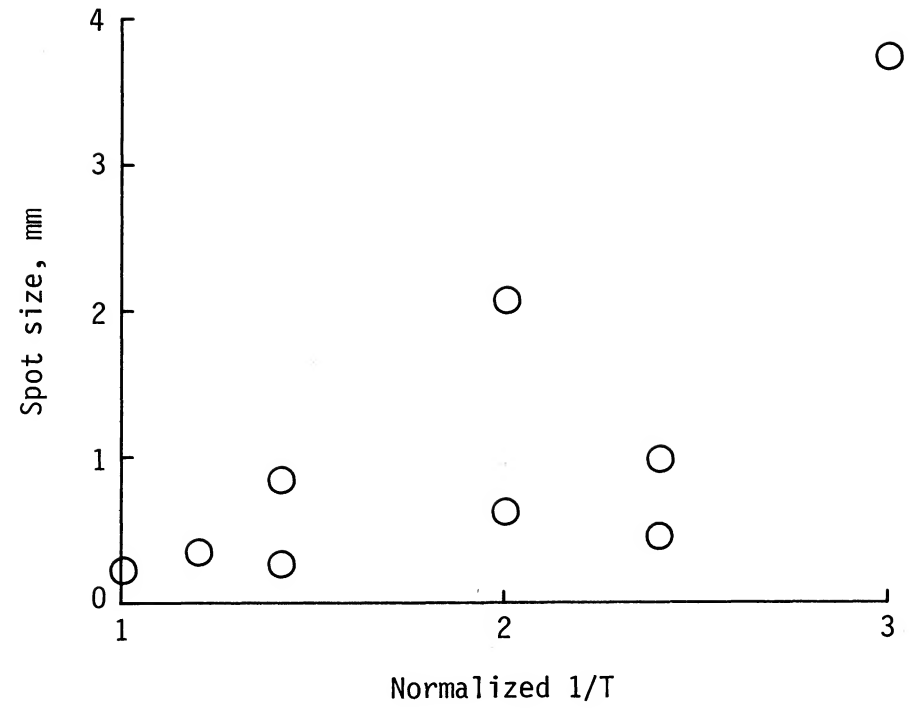

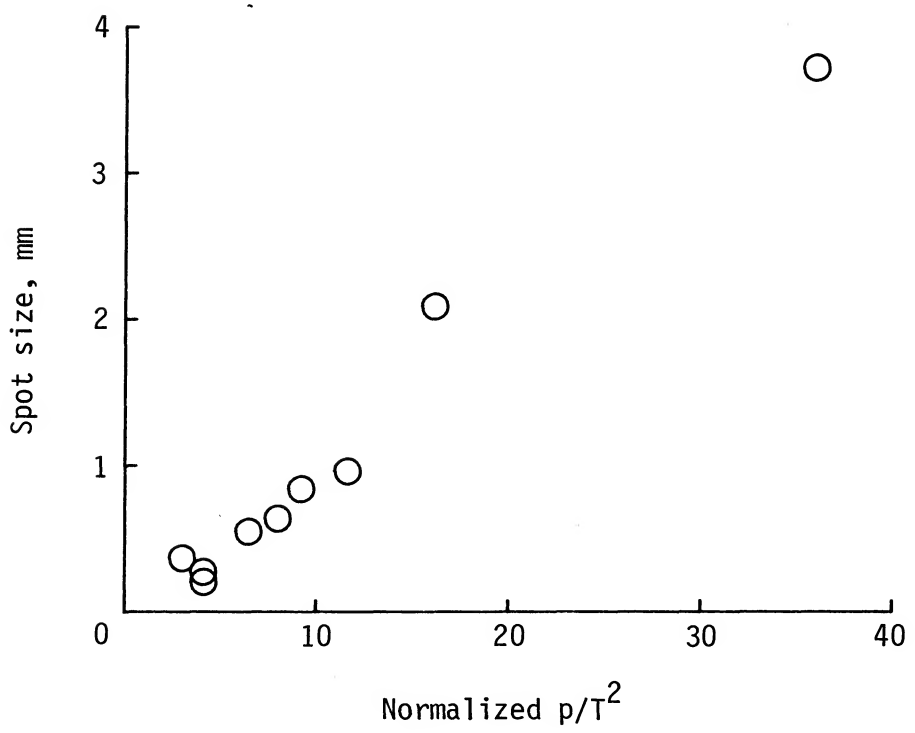

Figure 13.- Spot size of reconstructed images plotted against 1/T and p/T^2. Curves are normalized to 300 K and 1 atm.

1. Report No.	2. Government Accession No.	3. Recipient's Catalog No.
NASA TM-84556		

4. Title and Subtitle	5. Report Date
FLOW VISUALIZATION IN A CRYOGENIC WIND TUNNEL USING HOLOGRAPHY	November 1982
	6. Performing Organization Code: 505-31-53-06
7. Author(s): A. W. Burner and W. K. Goad	8. Performing Organization Report No.: L-15510
	10. Work Unit No.
9. Performing Organization Name and Address: NASA Langley Research Center, Hampton, VA 23665	11. Contract or Grant No.
	13. Type of Report and Period Covered: Technical Memorandum
12. Sponsoring Agency Name and Address: National Aeronautics and Space Administration, Washington, DC 20546	14. Sponsoring Agency Code

15. Supplementary Notes

16. Abstract

Results of holographic flow visualization are presented from tests made in the Langley 0.3-Meter Transonic Cryogenic Tunnel which was operated over a temperature range from 100 to 300 K and a pressure range from 1.1 to 4 atm. Interferometry at the facility may be of limited use at the low-temperature—high-pressure conditions because of the jumbled nature of the reference fringes. The shadowgraph technique appears to be the best means of visualizing shocks at these high-density conditions. The spot size at the focus of the recontructed beams was measured and used as an indicator of density fluctuations in the flow field. These density fluctuations appear to be caused by temperature fluctuations of the test gas which are relatively independent of tunnel conditions.

17. Key Words (Suggested by Author(s))	18. Distribution Statement
Flow visualization Cryogenic wind tunnels Holography	Unclassified - Unlimited Subject Category 35

19. Security Classif. (of this report)	20. Security Classif. (of this page)	21. No. of Pages	22. Price
Unclassified	Unclassified	20	A02

For sale by the National Technical Information Service, Springfield, Virginia 22161

NASA-Langley, 1982